1064 *KSME International Journal, Vol. 12, No. 6, pp. 1064~1072, 1998*

Kinematic Analysis of the Wire Parallel Mechanism for Full Coordinate Measuring of Industrial Robot

Jae Won Jeong*, Soo Hyun Kim* and Yoon Keun Kwak*

(Received January 13, 1998)

This paper presents a wire parallel mechanism for full coordinate measuring of industrial robot. The mechanism is constructed with six parallel wires that act as links. The position and orientation of a robot end-effector are obtained from the wire lengths. The equations of the forward kinematics are solved by a Newton-Raphson method, and the unique solution is determined from the geometric configuration of the mechanism. A method to estimate the workspace is presented. Through simulations, it is verified that the proposed mechanism can measure a robot pose over a large workspace, and can be used effectively for full coordinate measuring of a robot with little cost and effort.

Key Words: Robotics, Forward Kinematics, Numerical Analysis, Full Coordinate Measuring , Wire Parallel Mechanism, Measuring Space

1. Introduction

Coordinate measurements of the position and orientation of an industrial robot are necessary for calibrate to compensation for parameter error of the robot to improve accuracy.

Systems for measuring a robot pose include theodolite(Whitney, 1986; Judd, 1990), laser system(Gilby, 1982), LineAr Variable Differential Transformer(LVDT) (Zupancic, 1994), Coordinate Measuring Machine(CMM) (Renders, 1991; Everett, 1995) and vision(Van Albada, 1995; Driels, 1991) *etc.*

However, these methods have limited accuracy and have difficulty sensing six degrees of freedom simultaneously. Laser systems and CMM have a high accuracy($\pm$0.1mm~0.1μm), but are very sensitive to the environment and have difficulty with simultaneous multiple degrees of freedom. A theodolite is very cumbersome to use, and vision systems have low accuracy($\pm$0.1mm) and are usually limited to three degrees of freedom measurements.

Any method for measuring a robot pose should satisfy the performance criteria suggested in ISO 9283 and 9946. Inagaki *et al.* (1989) indicate that to satisfy the above criteria will require the pose measuring device to identify six degrees of freedom with good accuracy and resolution in an efficient and cost effective manner.

Studies on a multiple degree of freedom mechanism using wires have been done recently. Ming (1990) has proposed the relationship between the degrees of freedom and the number of wires, while Kawamura *et al.* (1993) have used the wire in a master robot for teleoperation. Ming *et al.* (1994a, 1994b, 1995) have manufactured a wire parallel mechanism, called "OPT-FOLLOW", and have shown the feasibility of using wires through static and dynamic analyses. However the above mechanism is a Completely Restrained Wire Parallel Mechanism(CRWPM) that uses four wires to measure three degrees of freedom (x, y, ϕ); it has been shown that N+1 wires are required to measure N degrees-of-freedom.

In this paper, we propose a wire parallel mechanism for measuring the position and orientation of a robot end-effector. The mechanism is designed as a parallel mechanism with six wire links. The robot pose, that is the position and

* Department of Mechanical Engineering, Korea Advanced Institute of Science and Technology

orientation, is obtained from the forward kinematics using the six wire lengths. Also, a method to estimate the measuring space of the mechanism is presented.

2. Wire Parallel Mechanism

Figure 1 shows the proposed wire parallel mechanism for the full coordinate measuring of an industrial robot.

The pose of a robot, that is, the position and orientation of the center of the robot attachment, is calculated from the measured six wire lengths. The roll, pitch and yaw angles of the robot attachment are limited to within $\pm 90°$ about the referencing frame to prevent a tangle of the wires.

In Fig. 1, each end of the robot attachment, which can rotate about 3 axes(x, y and z), is connected by two wires. This "T" configured attachment is designed to determine the position of the center of the horizontal bar and the orientation from the vertical bar. To obtain a unique solution the forward kinematics, a level vial which can detect the incline direction is attached in the plane above the robot attachment. The wire length is measured by the encoder when the robot attachment moves.

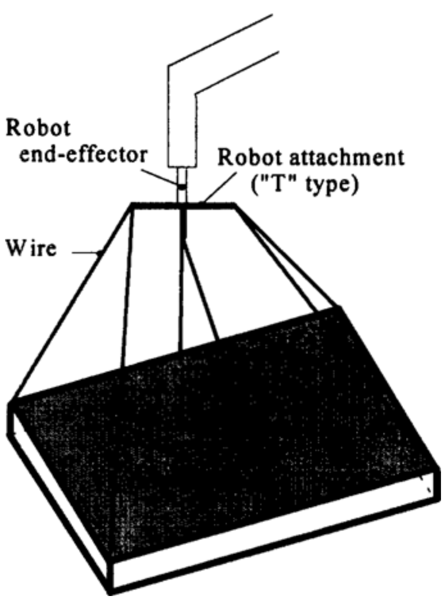

Fig. 1 The wire parallel mechanism for full coordinate measuring of industrial robot.

3. Kinematic Analysis

The forward kinematics of a parallel mechanism is more difficult to solve than the inverse kinematics. In the case of a Stewart platform, which is a typical parallel mechanism with six degrees of freedom, it is very difficult not only to solve the forward kinematics analytically but also to obtain a unique solution in a large workspace because of the high order nonlinear polynomials that occur.(Liu, 1993; Husain, 1994). In this paper, we are going to solve the forward and inverse kinematics using the wire lengths measured in the parallel wire mechanism, and determine the unique solution based on the geometric configuration of the mechanism.

In Fig. 2, it is straightforward to determine the wire lengths, $l_i(i=1\sim6)$, as follows:

$$x_1^2+y_1^2+z_1^2=l_1^2 \tag{1}$$
$$x_1^2+(y_1-b)^2+z_1^2=l_2^2 \tag{2}$$
$$(x_3-a/2)^2+y_3^2+z_3^2=l_3^2 \tag{3}$$
$$(x_3-a/2)^2+(y_3-b)^2+z_3^2=l_4^2 \tag{4}$$
$$(x_2-a)^2+y_2^2+z_2^2=l_5^2 \tag{5}$$
$$(x_2-a)^2+(y_2-b)^2+z_2^2=l_6^2 \tag{6}$$

where (x, y, z), (x_1, y_1, z_1), (x_2, y_2, z_2) and (x_3, y_3, z_3) are the coordinates of P, P_1,

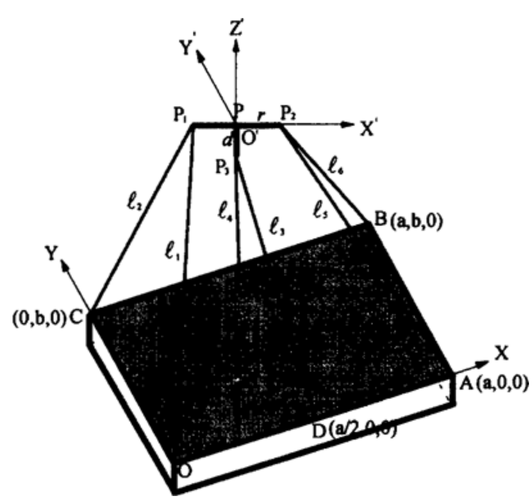

Fig. 2 Analytic model of the wire parallel mechanism.

P_2 and P_3 respectively, a and b are the dimensions of the base plate, and r and d are $\overline{PP_2}(=\overline{PP_1})$ and $\overline{PP_3}$, respectively.

3.1 Inverse Kinematics

The analytic wire lengths, $l_i(i=1\sim6)$, can be determined from the coordinates of P_1, P_2 and P_3 in Eqs. (1)~(6). For now, $P_i(i=1\sim3)$, which are the coordinates of each end of the robot attachment, are obtained from the given coordinate, $\underline{P}$, about the reference frame as below

$$\underline{P_i}=\underline{P}+R_{\phi,\theta,\psi}{}^u\underline{P_i}(i=1,2,3) \tag{7}$$

where ${}^u\underline{P_i}$ represents the position of each end of the robot attachment in the body frame $(O'X'Y'Z')$, and $R_{\phi,\theta,\psi}$ is the rotation matrix about the reference frame.

3.2 Forward Kinematics

The forward kinematics is the mapping from the wire lengths, $l_i(i=1\sim6)$, to the position and orientation of the robot attachment. From Eqns. (1)-(6) $y_i(i=1\sim3)$ can be determined as follows:

$$y=\frac{1}{2b}(l_1^2-l_2^2+b^2) \tag{8}$$

$$y_2=\frac{1}{2b}(l_5^2-l_6^2+b^2) \tag{9}$$

$$y_3=\frac{1}{2b}(l_3^2-l_4^2+b^2) \tag{10}$$

Substituting Eqs. (8)~(10) into Eqs. (1), (3) and (5), $z_i(i=1\sim3)$ can be expressed in terms of only the wire lengths and the $x_i(i=1\sim3)$:

$$z_1=\pm\sqrt{l_1^2-x_1^2-\left\{\frac{1}{2b}(l_1^2-l_2^2+b^2)\right\}^2} \tag{11}$$

$$z^2=\pm\sqrt{l_5^2-(x_2-a)^2-\left\{\frac{1}{2b}(l_5^2-l_6^2+b^2)\right\}^2} \tag{12}$$

$$z_3=\pm\sqrt{l_3^2-\left(x_3-\frac{a}{2}\right)^2-\left\{\frac{1}{2b}(l_3^2-l_4^2+b^2)\right\}^2} \tag{13}$$

The coordinates of P_1, P_2 and P_3 must also satisfy the constraints

$$(x_1-x_2)^2+(y_1-y_2)^2+(z_1-z_2)^2=4r^2 \tag{14}$$

$$(x_1-x_3)^2+(y_1-y_3)^2+(z_1-z_3)^2=r^2+d^2 \tag{15}$$

$$(x_2-x_3)^2+(y_2-y_3)^2+(z_2-z_3)^2=r^2+d^2 \tag{16}$$

Substituting Eqs. (8)~(13) into Eqs. (14)~(16) yields three nonlinear algebraic equations in three variables (x_1, x_2, x_3):

$$-2x_1x_2+2ax_2-2\sqrt{(A-x_1^2)\{B-(x_2-a)^2\}}-2\sqrt{(A-l_1^2)(B-l_5^2)}-a^2-4r^2+l_1^2+l_5^2=0 \tag{17}$$

$$-2x_1x_3+ax_3-2\sqrt{(A-x_1^2)\left\{C-\left(x_3-\frac{a}{2}\right)^2\right\}}-2\sqrt{(A-l_1^2)(C-l_3^2)}-\frac{1}{4}a^2-r^2-d^2+l_1^2+l_3^2=0 \tag{18}$$

$$-2x_2x_3+2ax_2+ax_3-2\sqrt{\{B-(x_2-a)^2\}\left\{C-\left(x_3-\frac{a}{2}\right)^2\right\}}-2\sqrt{(B-l_5^2)(C-l_3^2)}-\frac{5}{4}a^2-r^2-d^2+l_3^2+l_5^2=0 \tag{19}$$

where

$$A=l_1^2-\frac{1}{4b^2}(l_1^2-l_2^2+b^2)$$

$$B=l_5^2-\frac{1}{4b^2}(l_5^2-l_6^2+b^2)$$

$$C=l_3^2-\frac{1}{4b^2}(l_3^2-l_4^2+b^2)$$

Since Eqs. (17)~(19) are highly nonlinear simultaneous equations, it is in general impossible to solve them explicitly, and only numerical solutions can be obtained. In this paper, the Newton-Raphson method is used, which converges quadratically in the vicinity of a solution.

3.3 Determination of the Unique Solution

Eqs. (17)~(19) can be rewritten as

$$f_{12}(x_1, x_2)=0 \tag{20}$$

$$f_{13}(x_1, x_3)=0 \tag{21}$$

$$f_{23}(x_2, x_3)=0 \tag{22}$$

with only two variables involved in each of the f_{ij}. Since the highest order of each f_{ij} is two, there may exist up to eight sets of (x_1, x_2, x_3) that satisfy the nonlinear equations (20)~(22). Because the measuring range($\pm90°$) of the roll, pitch and yaw angles about the reference frame must be considered, $x_1\leq x_2$. Thus only two solutions of the eight satisfy the range of the configuration.

To extract the unique solution from the two possible solutions within the allowable range, a level vial is used to determine the sign of the difference $z_1 - z_2$. Figure 3 illustrates that the two solutions can be differentiated by the sign of this difference $(z_1 - z_2)$ when $y_1 = y_2 = y_3$.

In Fig. 3, l_{ij} is a virtual length determined by l_i and l_j as follows:

$$l_{12} = l_1 \sqrt{1 - \left(\frac{l_1^2 + b^2 - l_2^2}{2bl_1} \right)^2} \tag{23}$$

$$l_{34} = l_3 \sqrt{1 - \left(\frac{l_3^2 + b^2 - l_4^2}{2bl_3} \right)^2} \tag{24}$$

$$l_{56} = l_5 \sqrt{1 - \left(\frac{l_5^2 + b^2 - l_6^2}{2bl_5} \right)^2} \tag{25}$$

Accordingly, the position of the robot attachment is calculated from the coordinates of P_1, P_2, and P_3, which are obtained from Eqs. (8) ~ (13):

$$x = \frac{1}{2}(x_1 + x_2) \tag{26}$$

$$y = \frac{1}{2}(y_1 + y_2) \tag{27}$$

$$z = \frac{1}{2}(z_1 + z_2) \tag{28}$$

Meanwhile, since the direction vector $\underline{X'}$ and $\underline{Z'}$ can be represented as

$$\underline{X'} = \frac{1}{\| \underline{P_2} - \underline{P} \|} (\underline{P_2} - \underline{P}) \tag{29}$$

$$\underline{Z'} = \frac{1}{\| \underline{P} - \underline{P_3} \|} (\underline{P} - \underline{P_3}), \tag{30}$$

the unknown direction vector $\underline{Y'}$ is calculated by the right hand rule as follow:

$$\underline{Y'} = \underline{Z'} \times \underline{X'} \tag{31}$$

So in terms of the rotation matrix $R_{Z,\phi} R_{Y,\theta} R_{X,\Psi}$ for roll, pitch and yaw angles, Eqs. (29) ~ (31) must satisfy the following:

$$\begin{bmatrix} X'_x & Y'_x & Z'_x \\ X'_y & Y'_y & Z'_y \\ X'_z & Y'_z & Z'_z \end{bmatrix} =$$

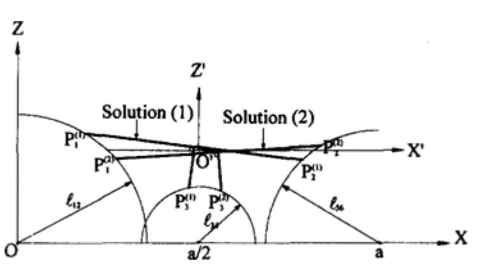

Fig. 3 The solutions of the robot attachment ("T" type) when $y_1 = y_2 = y_3$.

$$\begin{bmatrix} C_\phi C_\theta & C_\phi S_\theta S_\psi - S_\phi C_\psi & C_\phi S_\theta C_\psi + S_\phi S_\psi \\ S_\phi C_\theta & S_\phi S_\theta S_\psi + C_\phi C_\psi & S_\phi S_\theta C_\psi - C_\phi S_\psi \\ -S_\theta & C_\theta S_\psi & C_\theta C_\psi \end{bmatrix} \tag{32}$$

where $C_i = \cos(i)$, $S_i = \sin(i)$.

Therefore the roll, pitch and yaw angles, ϕ, θ, and Ψ, of the robot attachment are determined as follow:

$$\phi = A\tan 2\left(\frac{X'_y}{X'_x} \right) \tag{33}$$

$$\theta = A\tan 2\left(\frac{-X_z^2}{\sqrt{1 - X_z'^2}} \right) \tag{34}$$

$$\Psi = A\tan 2\left(\frac{Y'_z}{Z'_z} \right) \tag{35}$$

4. Measuring Space Analysis

The measuring space of the proposed wire parallel mechanism is limited by the wire lengths and the rotation range of the wire group connected with the base plate.

4.1 X-Z plane

The measuring space in the X-Z plane is determined by P_1 and P_2, and is maximized when $y_1 = y_2 = y_3$. Figure 4 shows the model for measuring space analysis in X-Z plane; we analyzed only five zones among the eight zones since it is symmetric about the $x = a/2$ line.

In Fig. 4, α and β are the angles between l_{12} and l_{56} to the base plate, respectively, α_{min} and β_{min} are the minimum angles of α and β limited by the wire group, respectively. Then l_{ij} have a

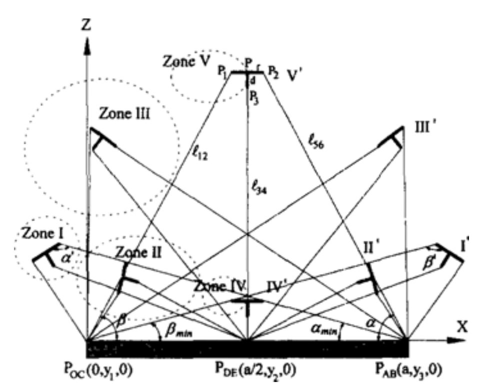

Fig. 4 The model for measuring space analysis in X -Z plane.

Table 1 List of constrained conditions and variables in each zones.

Zone	Constrained conditions	Variables
I (I')	$l_{56}=l_{56,\max}$, $\alpha=\alpha_{\min}$ ($l_{12}=l_{12,\max}$, $\beta=\beta_{\min}$)	$\alpha'(\beta')$
II (II')	$\alpha=\alpha_{\min}$, $\alpha'=90°$ ($\beta=\beta_{\min}$, $\beta'=90°$)	$l_{56}(l_{12})$
III (III')	$l_{56}=l_{56\max}(l_{12}=l_{12,\max})$	$\alpha(\beta)$
IV (IV')	$\alpha=\alpha_{\min}$, $\beta=\beta_{\min}$	$l_{56}(l_{12})$
V (V')	$l_{12}=l_{12,\max}$, $l_{56}=l_{56,\max}$	$\alpha(\beta)$

maximum value when $l_{i,\max}=l_{j,\max}$. Table 4 shows the constraint conditions and variables in each zone of Fig. 4.

A. Zone I

This zone has a region of $\alpha'=[90°, 180°]$ under the condition $\alpha=\alpha_{\min}$ and $l_{56}=l_{56,\max}$. P is calculated as follows:

$$x=a-\overline{PP_{AB}}\cos\{\alpha_{\min}-\text{Atan2}(S_I,C_I)\} \quad (36)$$

$$z=\overline{PP_{AB}}\sin\{\alpha_{\min}-\text{Atan2}(S_I,C_I)\} \quad (37)$$

where

$$S_I=\frac{r}{\overline{PP_{AB}}}\sin\alpha',\ C_I=\sqrt{1-S_I^2}$$

$$\overline{PP_{AB}}=\sqrt{l_{56,\max}^2+r^2-2rl_{56,\max}\cos\alpha'}$$

B. Zone II

This zone has a region from $l_{56}=l_{56,\max}$ to $\beta=\beta_{\min}$ in condition of $\alpha=\alpha_{\min}$ and $\alpha'=90°$, P is calculated by varying l_{56} as follows:

$$x=a-\overline{PP_{AB}}\cos\{\alpha_{\min}-A\tan 2(r,\ l_{56})\} \quad (38)$$

$$z=\overline{PP_{AB}}\sin\{\alpha_{\min}-A\tan 2(r,\ l_{56})\} \quad (39)$$

Then, l_{56}, when $\beta=\beta_{\min}$, is obtained from Eq. (40) by an iteration method:

$$\beta=180°-A\tan 2(S_{II},\ C_{II}) \quad (40)$$

where

$$S_{II}=\sqrt{4r^2+l_{56}^2}\sin\{\alpha_{\min}-A\sin 2(2r,\ l_{56})\}$$

$$S_{II}=\sqrt{4r^2+l_{56}^2}\cos\{\alpha_{\min}-A\tan 2(2r,\ l_{56})\}-a$$

C. Zone III

This zone has a region from $\alpha=\alpha_{\min}$ to $l_{12}=l_{12,\max}$ in condition of $l_{56}=l_{56,\max}$ and $\alpha'=180°$. P is calculated by varying α.

$$x=a-(l_{56,\max}+r)\cos\alpha \quad (41)$$

$$z=(l_{56,\max}+r)\sin\alpha \quad (42)$$

Then, α, when $l_{12}=l_{12,\max}$, can be obtained from Eq. (43):

$$\alpha=A\tan 2(S_{III},\ S_{III}) \quad (43)$$

where

$$C_{III}=\frac{(l_{56,\max}+2r)^2-l_{12,\max}^2+a^2}{2a(l_{56,\max}+2r)}$$

$$S_{III}=\sqrt{1-C_{III}^2}$$

D. Zone IV

This zone has a region from $\alpha'=90°$ to $x=a/2$ in condition of $\alpha=\alpha_{\min}$ and $\beta=\beta_{\min}$. $P$is calculated by varying l_{56}.

$$x=a-\overline{P_{AB}P}\cos\{\alpha_{\min}-A\tan 2(S_{IV},\ C_{IV})\} \quad (44)$$

$$z=\overline{P_{AB}P}\sin\{\alpha_{\min}-A\tan 2(S_{IV},\ C_{IV})\} \quad (45)$$

where

$$\overline{P_{AB}P}=\sqrt{r^2+l_{56}^2-2rl_{56}\cos\alpha'}$$

$$S_{IV}=\frac{r}{\overline{P_{AB}P}}\sin\alpha',\ C_{IV}=\sqrt{1-S_{IV}^2}$$

$$\alpha'=180-(\alpha_{\min}+\beta_{\min})-A\tan 2(S_{IV,1},\ C_{IV,1})$$

$$S_{IV,1}=\frac{\overline{P_{OC}P_2}}{2r}\sin\{A\tan 2(S_{IV,2},\ C_{IV,2})-\beta_{\min}\},$$

$$C_{IV,1}=\sqrt{1-S_{IV,1}^2}$$

$$S_{IV,2}=\frac{l_{56}}{\overline{P_{OC}P_2}}\sin\alpha_{\min},\ C_{IV,2}=\sqrt{1-S_{IV,2}^2}$$

$$\overline{P_{OC}P_2}=\sqrt{l_{56}^2+a^2-2al_{56}\cos\alpha_{\min}}$$

The initial value of l_{56} is determined from Eq. (40). l_{56}, when $x=a/2$, is obtained as follows:

$$l_{56,x=a/2}=\frac{(a-2r)\tan\beta_{\min}}{\sin\alpha_{\min}+\cos\alpha_{\min}\tan\beta_{\min}}.$$

E. Zone V

This zone is a region determined by varying α in condition of $l_{12}=l_{12,\max}$ and $l_{56}=l_{56,\max}$. The initial value of α is obtained from Eq. (43) of zone III, α, when $x=a/2$, can be obtained from ($2l_{56,\max}\cos\alpha=a-2r$). Therefore P is calculated as follows:

$$x=\frac{1}{2}(l_{12,\max}\cos\beta-l_{56,\max}\cos\alpha+a) \quad (46)$$

$$z = \frac{1}{2}(l_{12,\max}\sin\beta + l_{56,\max}\sin\alpha) \tag{47}$$

where

$$\beta = A\tan 2(S_{V,1}, C_{V,1}) + A\tan 2(S_{V,2}, S_{V,2})$$

$$C_{V,1} = \frac{1}{2 l_{12,\max}\overline{P_{OC}P_2}}(l_{12,\max}{}^2 + \overline{P_{OC}P_2}{}^2 - 4r^2),$$

$$S_{V,1} = \sqrt{1 - C_{V,1}{}^2}$$

$$S_{V,2} = \frac{l_{56,\max}}{\overline{P_{OC}P_2}}\sin\alpha, \quad C_{V,2} = \sqrt{1 - S_{V,2}{}^2}$$

$$\overline{P_{OC}P_2} = \sqrt{a^2 + l_{56,\max}{}^2 - 2a l_{56,\max}\cos\alpha}$$

4.2 Y-Z plane

The measuring space in the Y-Z plane is determined by P_3, and it is a maximized when $y_1 = y_2 = y_3$ and $x_3 = a/2$. Figure 5 shows the model for measuring space analysis in the Y-Z plane.

A. Zone I

This zone has a region of $\alpha = \left[\alpha_{\min}, A\tan 2\left(l_{34,\max}, \sqrt{l_{3,\max}{}^2 - l_{34,\max}{}^2}\right)\right]$ in condition of $l_3 = l_{3,\max}$. P is calculated as follows:

$$y = (l_{3,\max} + d)\cos\alpha \tag{48}$$

$$z = (l_{3,\max} + d)\sin\alpha \tag{49}$$

B. Zone II

This zone has a region of $\gamma' = [0, \alpha_{\min}]$ in condition of $l_3 = l_{3,\max}$. P is calculated as follows:

$$y = l_{3,\max}\cos\alpha_{\min} + d\cos\gamma' \tag{50}$$

$$y = l_{3,\max}\sin\alpha_{\min} + d\sin\gamma' \tag{51}$$

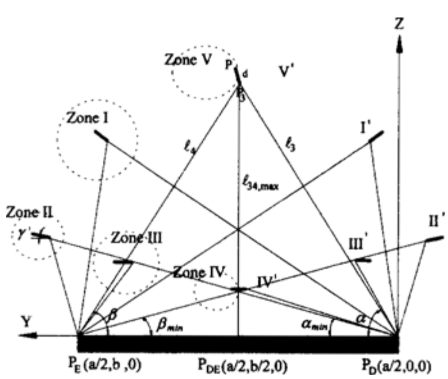

Fig. 5 The model for measuring space analysis in the Y-Z plane.

C. Zone III

This zone has a region from $l_3 = l_{3,\max}$ to $y_3 = b/2$ in condition of $\gamma' = 0°$ and $\alpha = \alpha_{\min}$. P is calculated by varying l_3 as follows:

$$y = l_3\cos\alpha_{\min} + d \tag{52}$$

$$z = l_3\sin\alpha_{\min} \tag{53}$$

Then, l_3, when $y_3 = b/2$, is calculated as follows:

$$l_{3,y_3=b/2} = b\left(\frac{\tan\beta_{\min}}{\cos\alpha_{\min}\tan\beta_{\min} + \sin\alpha_{\min}}\right)$$

D. Zone IV

This zone has a region from $y_3 = b/2$ to $y = b/2$ having the same configuration with Zone III. $P$is calculated by varying l_4:

$$y = b - l_3\cos\beta_{\min} + d \tag{54}$$

$$z = l_4\sin\beta_{\min} \tag{55}$$

Then $l_{4,y3=b/2}$ and $l_{4,y=b/2}$ are calculated as follows:

$$l_{4,y_3=b/2} = b\left(\frac{\sin\alpha_{\min}}{\sin(\alpha_{\min} + \beta_{\min})}\right)$$

$$l_{4,y=b/2} = l_{4,y_3=b/2} + (d/\cos\beta_{\min})$$

E. Zone V

This zone has a region $\gamma' = [\alpha, 90°]$ in condition of $y_3 = b/2$, $l_3 = l_{3,\max}$, and $l_4 = l_{4,\max}$. P is calculated as follows:

$$y = l_{3,\max}\cos\alpha + d\cos\gamma' \tag{56}$$

$$z = l_{3,\max}\sin\alpha + d\sin\gamma' \tag{57}$$

where

$$\alpha = A\tan 2\left(l_{34,\max}, \sqrt{l_{3,\max}{}^2 - l_{34,\max}{}^2}\right)$$

Table 2 Specifications of the wire parallel mechanism for simulations.

Description	Value
Dimension of the base plate($a \times b$)	$500 \times 500 mm$
Dimension of the "T" type($r \times d$)	50×50mm
Maximum wire length($l_{i,\max}$, $i = 1, \cdots, 6$)	$1000 mm$
Minimum angle of the wire group($\alpha_{\min}$,$\beta_{\min}$)	40°
Measuring resolution of wire	2μm

5. Simulations

Table 2 shows the specifications of the wire parallel mechanism used for simulations.

5.1 Kinematic analysis

The equations and method olosy were verified using three cases specified by the position and orientation, $P(x, y, z, \Psi, \theta, \phi)$ as shown below:

Case 1 : P(270.000, 330.000, 600.000, 0.0°, 0.0°, 36.87°)

Case 2 : P(180.000, 150.000, 750.000, 25.0°, 10.0°, 0.0°)

Case 3 : P(250.000, 250.000, 500.000, 40.0°, 50.0°, 60.0°)

where the units of x, y, z are mm, the units of Ψ, θ, ϕ, which are roll, pitch and yaw angles, are *degrees*. The inverse kinematics is calculated from Eqs. (1)-(7) and listed in Table 3.

Table 3 The solutions of inverse kinematics.

unit : mm

	Case 1	Case 2	Case 3
l_1	709.154	784.345	627.575
l_2	672.978	845.693	649.372
l_3	641.716	730.000	534.518
l_4	576.021	782.157	543.185
l_5	725.052	803.345	587.435
l_6	644.748	863.344	563.246

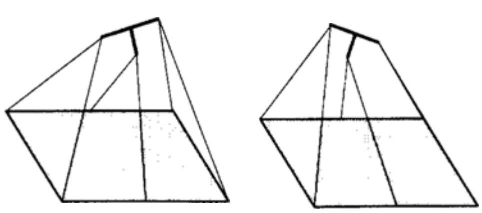

(a) $(Z_1-Z_2)<0$ (b) $(Z_1-Z_2)>0$

Fig. 6 Comparison of the solutions in the Case 2.

Table 4 shows the solutions of the forward kinematics obtained from Eqs. (17)-(35) using the results of Table 3.

From the solutions derived in Table 4, we can see that the unique solution can be determined by

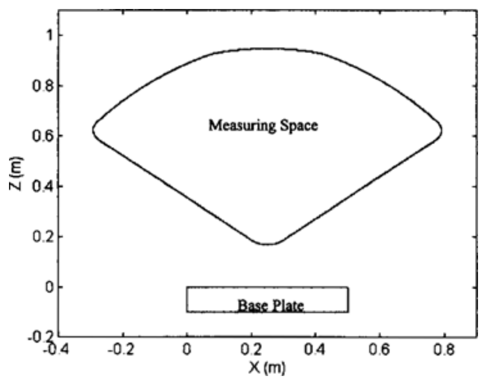

Fig. 7 Measuring space of the wire parallel mechanism in X-Z plane.

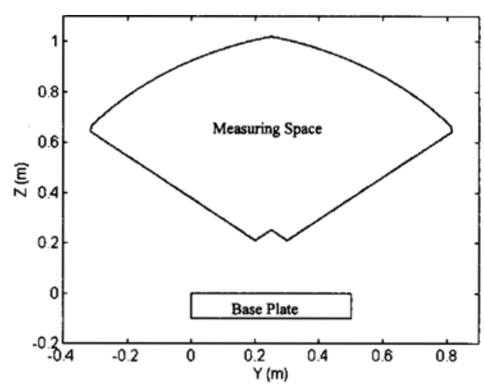

Fig. 8 Measuring space of the wire parallel mechanism in Y-Z plane.

Table 4 The solutions of forward kinematics.

Case	Z_1-Z_2	Position (mm)	Euler angles (*degree*)
1	0	**(270.001, 330.000, 600.000)**	**(−0.007, 0.0, 36.870)**
2	−	(263.180, 150.000, 752.740)	(24.999, −15.932, 0.0)
	+	**(180.000, 150.000, 750.000)**	**(24.998, 10.000, 0.0)**
3	−	(378.050, 250.000, 494.690)	(−26.153, −18.767, 36.007)
	+	**(250.000, 250.000, 500.000)**	**(39.995, 50.001, 59.996)**

choosing the inclined direction of the level vial, that is the sign of z_1-z_2. Figure 6 show the solutions having the robot attachment for Case 2.

5.2 The measuring space

From the specifications of Table 2, $l_{12,max}$, $l_{34,max}$ and $l_{56,max}$ are calculated as follows:

$l_{12,max}=968.246(mm)$, $l_{34,max}=968.246(mm)$, $l_{56,max}=968.246(mm)$

The measuring space in the X-Z plane and Y-Z plane are shown in Fig. 7 and Fig. 8, respectively.

6. Conclusions

This paper proposed a wire parallel mechanism for the full coordinate measuring of industrial robots. The nonlinear equations of the forward kinematics of a parallel mechanism are solved by the Newton-Raphson method, and the unique solution is determined from the geometric configuration of the mechanism. Through a measuring space analysis for the proposed mechanism, we confirmed that this wire parallel mechanism has a large measuring space. In conclusion, we believe that this mechanism is useful for full coordinate measuring for kinematic parameter error compensation of industrial robots.

References

Driels, M. R. and Pathre, U. S., 1991, "Vision-Based Automatic Theodolite for Robot Calibration," *IEEE Trans. on Robotics and Automation,* Vol. 7, No. 3, pp. 351~360.

Everett, L. J. and Lei, J., 1995, "Improved Manipulator Performance Through Local D-H Calibration," *J. of Robotic Systems,* Vol. 12, No. 7, pp. 505~514.

Gilby, J. H. and Parker, G. A., 1982, "Laser tracking system to measure robot arm performance," *Sensor Review,* Vol. 2, No. 4, pp. 180~184.

Husain, M. and Waldron, K. J. , 1994, "Direct Position Kinematics of the 3-1-1-1 Stewart Platforms," *ASME J. of Mechanical Design,* Vol. 116, pp. 1102~1107.

Inagaki, S. , Ando, Y. and Suzuki, S., 1989, "Characteristics of Measuring Equipment for Manipulating Industrial Robots," *20th Int. Symp. On Industrial Robots,* Japan, pp. 987~992.

Judd, R. P. and Knasinsk, A. B., 1990, "A Techinique to Calibrate Industrial Robots with Experimental Verification," *IEEE Trans. on Robotics and Automation,* Vol. 6, No. 1, pp. 20~30.

Kawamura, S. and Ito, K., 1993, "A New Type of Master Robot for Teleoperation Using a Radial Wire Drive System," *Proc. 1993 IEEE/RSJ Int. Conf. Intelligent Robots and systems,* Japan, pp. 55~60.

Liu, K. , Fitzgerald, J. and Lewis, F. L., 1993, "Kinematic Analysis of a Stewart Platform Manipulator," *IEEE Trans. on Industrial Electronics,* Vol. 40, No. 2, pp. 282~293.

Ming, A., 1990, *Study on Multiple Degree-of-Freedom Positioning Mechanism Using Wires,* Ph. D. Thesis, University of Tokyo, Japan.

Ming, A. and Higuchi, T., 1994, "Study on Multiple Degree-of-Freedom Positioning Mechanism Using Wires(Part 1)-Concept, Design and Control-," *Int. J. JSPE,* Vol. 28, No. 2, pp. 131~138.

Ming, A. and Higuchi, T., 1994, "Study on Multiple Degree-of-Freedom Positioning Mechanism Using Wires(Part 2)-Development of Planar Completely Restrained Positioning Mechanism-," *Int. J. JSPE,* Vol. 28, No. 3, pp. 235~242.

Ming, A., Kajitani, M. and Higuchi, T., 1995, "On the Design of Wire Parallel Mechanism," *Int. J. JSPE,* Vol. 29, No. 4, pp. 337~342.

Renders, J. M., Rossignol, E. , Becquet, M. and Hanus, R. , 1991, "Kinematic Calibration and Geometrical Parameter Identification for Robots," *IEEE Trans. on Robotics and Automation,* Vol. 7, No. 6, pp. 721~732.

Van Albada, G. D., Lager, J. M., Visser, A. and Hertzberger, L. O., 1995, "A low-cost pose-measuring system for robot calibration," *Robotics and Autonomous Systems,* Vol. 15, pp. 207~227.

Whitney, D. E. , Lozinski, C. A. and Rourke, J. M. , 1986, "Industrial Robot Forward Calibration Method and Results," *ASME J. of Dynamic Systems, Measurement and Control,* Vol. 108, pp. 1～8.

William, H. P., Saul, A. T., William, T. V. and Brian, P. F., 1992, *Numerical Recipes in C-The Art of Scientific Computing -2nd Edition-,* Cambridge Uni. press, New York, pp. 379～383.

Zupancic, J., 1994, "Calibration of an SMT Robot Assembly Cell," *J. of Robotics Systems,* Vol. 11, No. 4, pp. 301～310.